Industrial Chemistry & Materials

ROYAL SOCIETY OF CHEMISTRY

MINI REVIEW

View Article Online
View Journal | View Issue

Cite this: *Ind. Chem. Mater.*, 2023, **1**, 376

Hierarchically microporous membranes for highly energy-efficient gas separations

Shuangjiang Luo, [a] Tianliang Han,[a] Can Wang,[a] Ying Sun,[a] Hongjun Zhang, [b] Ruilan Guo *[c] and Suojiang Zhang *[ade]

The implementation of synthetic polymer membranes in gas separations, ranging from natural gas sweetening, hydrogen separation, helium recovery, carbon capture, oxygen/nitrogen enrichment, *etc.*, has stimulated the vigorous development of high-performance membrane materials. However, size-sieving types of synthetic polymer membranes are frequently subject to a trade-off between permeability and selectivity, primarily due to the lack of ability to boost fractional free volume while simultaneously controlling the micropore size distribution. Herein, we review recent research progress on microporosity manipulation in high-free-volume polymeric gas separation membranes and their gas separation performance, with an emphasis on membranes with hourglass-shaped or bimodally distributed microcavities. State-of-the-art strategies to construct tailorable and hierarchically microporous structures, microporosity characterization, and microcavity architecture that govern gas separation performance are systematically summarized.

Received 28th November 2022,
Accepted 13th February 2023

DOI: 10.1039/d2im00049k

rsc.li/icm

Keywords: Gas separation membranes; Hierarchical microporosity; Micropore size distribution; Configurational free volume; Solution–diffusion mechanism.

[a] *CAS Key Laboratory of Green Process and Engineering, State Key Laboratory of Multiphase Complex Systems, Beijing Key Laboratory of Ionic Liquids Clean Process, Institute of Process Engineering, Chinese Academy of Sciences (CAS), Beijing 100190, China. E-mail: sjzhang@ipe.ac.cn*
[b] *State Key Laboratory of Particle Detection and Electronics, University of Science and Technology of China, Hefei 230026, China*
[c] *Department of Chemical and Biomolecular Engineering, University of Notre Dame, Notre Dame, IN 46556, USA. E-mail: rguo@nd.edu*
[d] *Longzihu New Energy Laboratory, Zhengzhou 450000, China*
[e] *Henan University, Jinming Road, Kaifeng, 475004, China*

Shuangjiang Luo

Shuangjiang Luo obtained his Ph.D. from the Institute of Chemistry, Chinese Academy of Sciences (ICCAS) in 2013. Following his post-doctoral experience in the Department of Chemical Engineering at the University of Notre Dame (USA) and the Advanced Membrane and Porous Materials Center at the King Abdullah University of Science and Technology (KAUST), he became a professor at the Institute of Process Engineering, Chinese Academy of Sciences (IPECAS) in 2019. His main research interests include membranes and membrane-mediated separation, fabrication and structure–property relationship of gas separation membranes, hollow fiber membranes and modules, membrane system integration and process design.

1 Introduction

Gas separation membranes, based predominantly on synthetic polymers, have attracted substantial attention in various chemical, environmental, and energy-demanding separations, such as natural gas sweetening (CO_2/CH_4), helium recovery from natural gas (He/CH_4), carbon capture (CO_2/N_2), hydrogen recovery (H_2/N_2, H_2/CH_4), and oxygen/nitrogen enrichment (O_2/N_2), due to the advantages of high energy efficiency, small footprint, relatively low investment, and ease of operation.[1–3] However, synthetic polymer membranes are subject to a trade-off between permeability and selectivity, known as the Robeson upper bounds first introduced in 1991 and later in 2008,[4,5] which were redefined in 2015 for H_2/N_2, H_2/CH_4, and O_2/N_2 gas pairs[6] and in 2019 for CO_2/N_2 and CO_2/CH_4 gas pairs.[7] Common synthetic polymer membranes feature a broad pore size distribution of free volume-based micropores; thus, the enhancement of gas permeability by manipulating a polymer structure often leads to a more significant permeability increase for larger gases than smaller ones, resulting in decreased selectivities. This phenomenon has been frequently observed in dense polymer membranes and could be attributed to the lack of ability to boost fractional free volume while simultaneously controlling the size distribution of free volumes.[8] In this regard, microporosity manipulation plays a crucial role in obtaining attractive membranes with outstanding gas separation performance.

Ideal gas separation membranes feature precise and uniform pore sizes, *i.e.*, very narrow pore size distribution,

which enables both high gas permeability and selectivity due to high microporosity and low tortuosity in such membranes. Crystalline membrane materials, such as metal–organic frameworks (MOFs)[9] and covalent organic frameworks (COFs),[10] offer effective ways to adjust pore architecture and obtain narrow pore size distributions, potentially resulting in high permeability and high selectivity. However, almost all synthetic polymer gas separation membranes exhibit amorphous structures with random chain packing and microcavity architecture; thereby, it remains a significant challenge to achieve uniform or very narrowly distributed micropores in synthetic polymer membranes *via* the pore fabrication methods used in inorganic membranes. Biological membranes, such as aquaporins and potassium ion channels, have extraordinarily high permeability–selectivity combinations (Fig. 1a).[8] This is ascribed to the unique hourglass-shaped cavities providing open spaces for fast molecule transport and narrow neck for highly selective molecule sieving (Fig. 1b). The concept of introducing hourglass-shaped microcavities has also attracted much attention in synthetic polymer gas separation membranes, and some high-performance gas separation membranes were also observed to have this kind of microcavity architecture. However, the practical development of these gas separation membranes is still in its infancy and hasn't been systematically reviewed. Besides, most recently published reviews of gas separation membranes focused on the macromolecular design and polymer synthesis strategies of polymers of intrinsic microporosity;[11–13] few highlighted the construction and manipulation of microcavity structures.

This review summarizes the research progress on microporosity manipulation in high-free-volume polymer gas separation membranes and their gas separation performance, with an emphasis on membranes with hourglass-shaped or bimodally distributed microcavities. Here, we propose the idea of "hierarchically microporous membranes" featuring both micropores (<2 nm) and ultra-micropores (<7 Å) with bimodal or multimodal microcavity size distributions, which are distinctly different from the broad microcavity size distributions of conventional polymer membranes. Microporosity characterization methods, construction strategies of hierarchically microporous membranes, and structure–property relationships are discussed and reviewed. Various applications of hierarchically microporous membranes are also presented.

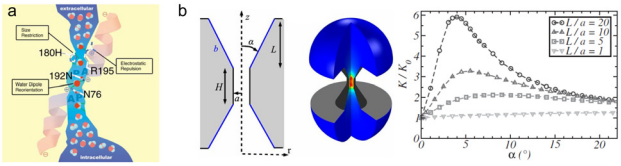

Fig. 1 (a) The sagittal cross-section of an aquaporin water channel (reprinted with permission from ref. 14, Copyright (2002) American Society for Clinical Investigation) and (b) the effect of the hourglass pore dimensional structure on water permeability (reprinted with permission from ref. 15, Copyright (2013) National Academy of Sciences).

2 Characterization of free volume

Various techniques have been employed to characterize microporosity in synthetic polymer membranes, including positron annihilation lifetime spectroscopy (PALS),[16] low-temperature gas adsorption (LTGA),[17] spin probe method,[18] inverse gas chromatography,[19] and molecular modeling.[20] Among them, PALS is frequently used to probe the microcavity size distribution of synthetic polymer membranes. The relatively easy operation have recently promoted the use of LTGA in measuring micropore size and pore size distribution.

Ruilan Guo

Prof. Ruilan Guo is the Frank M. Freimann Collegiate Associate Professor of Engineering at the University of Notre Dame (USA). Her research focuses on developing functional polymer membranes for gas separations and water treatment. Dr. Guo earned her Ph.D. from Georgia Tech (USA) and did postdoctoral research with Professor James McGrath at Virginia Tech (USA). She is a recipient of the U.S. Department of Energy Early Career Award, Inaugural Class of Influential Researchers by I&EC Research, and MSDE Emerging Investigator. She serves as an Editor of the journal Polymer and on the Editorial Advisory Board of Industrial Chemistry & Materials.

Suojiang Zhang

Prof. Suojiang Zhang is a Member of CAS. He is currently Director-General of the Institute of Process Engineering (IPE), CAS, Dean of College of Chemical Engineering, UCAS, and a Fellow of the Royal Society of Chemistry (RSC). He is mainly engaged in the research of green energy, materials and chemical processes, and has developed a number of new green media-enhanced reaction/separation technologies, and realizing the industrial application of a number of green complete technologies. He has published over 600 peer-reviewed articles and his publications have received more than 32 000 citations with an H-index of 92 (Google Scholar), authored 11 monographs.

2.1 Positron annihilation lifetime spectroscopy

Positron annihilation spectroscopy (PAS) has been demonstrated as an experimental instrumental technique to determine the free-volume (pore) properties of polymeric gas separation membranes. The positronium atom (Ps, a bound state of an electron and a positron, a quantum probe with a diameter of 0.106 nm) could be formed even in a subnanometer-scale pore with a diameter ranging from 1.5 to 7 Å (*i.e.*, ultra-micropore).[21] As the most commonly used PAS technique, positron annihilation lifetime spectroscopy (PALS) provides direct measurements of pore size, size distribution, and total pore fraction in polymeric gas separation membranes. A relationship exists between the *o*-Ps (the spin-triplet state of Ps) lifetime and the pore size, and the formation probability of *o*-Ps is correlated to the number of pores in a polymeric membrane. Using the CONTIN and MELT programs to analyze the PALS spectrum of a porous polymer, the size distribution of pores may also be obtained.

The age–momentum correlation (AMOC) of positron annihilation radiation provides valuable information on the chemical environment of the pore structure in the outermost layers of the membrane through analysis of the momentum distribution of long-lived *o*-Ps (the momentum of a thermalized positron is only approximately 0.025 eV at room temperature, far less than that of electrons). Additionally, using a variable mono-energetic positron beam (usually 0–30 keV), the depth-resolved porous structure (including porosity, pore connectivity, and chemical environment) of polymeric films in the depth range from the outermost layer to a maximum of ~10 μm can be revealed. Compared to the traditional gas absorption/desorption method, as discussed below, PAS possesses many apparent advantages in characterizing the microporous structures of polymeric membranes, as PAS experiments can be applied to polymeric membranes in various states: (1) as-prepared membranes but not broken powders (necessary for the gas absorption/desorption method); (2) wet-state membranes; (3) membranes at different temperatures (fixed temperature for the gas absorption/desorption method); and (4) membranes in different gases at different pressures.

Guo *et al.* used PALS to investigate the micropore size distribution of novel pentiptycene-based polyimides, and a bimodal micropore size distribution with average cavity sizes of 7–8 and 3–4 Å was observed. The microporous structure of these pentiptycene-based polyimide membranes was highly tailorable through the "partial filling" of the substituent groups in the pentiptycene moieties, as demonstrated by the PALS results.[22] Lee *et al.* revealed that the microporosity changed from a unimodal to a bimodal pore size distribution after the thermal rearrangement of hydroxyl-containing polyimide membranes. It was believed that the smaller 3–4 Å microcavities provided interconnections between the larger 6–8 Å micropores, which significantly enhanced gas permeabilities.[23] Additionally, the evolution of microporosity in thermally crosslinked membranes was also monitored by PALS. Luo *et al.* observed that dual thermally crosslinked polyimide membranes displayed a hierarchical micropore size distribution featuring ultra-micropore and micropore sizes in the range of 2–6 Å and 7–10 Å, respectively, which was different from the unimodal pore size distribution of the precursors. The dual thermally crosslinked polyimide membranes showed excellent plasticization resistance and low-temperature gas separation performance.[24]

2.2 Low-temperature gas adsorption

The low-temperature gas adsorption technique uses an inert gas (*e.g.*, N_2) that doesn't chemically adsorb onto an adsorbent as a probe to evaluate the surface area, average pore size, and pore size distribution of porous materials.[17,25,26] For most mesoporous materials with pore sizes in the range of 2–50 nm, the low-temperature N_2 adsorption can achieve reliable data due to their high enough adsorbing amounts. However, it usually takes too much time to obtain valuable data for pore size analysis of microporous (pore size <2 nm) materials. In this case, CO_2 is more frequently used to investigate the free volume and intrinsic microporosity in cellular materials due to the much shorter adsorption equilibrium time at 273.15 K.[27] Therefore, appropriate testing conditions and using adequate samples with repeated measurements are crucial for acquiring reliable pore structure data using this technique. Low-temperature adsorption has been widely used to probe micropore characteristics, including the intrinsic Brunauer–Emmett–Teller (BET) surface area, micropore size distribution, and gas storage capacity.[27] Pinnau *et al.* studied the microcavity size distribution of a series of triptycene-based polymers of intrinsic microporosity using low-temperature nitrogen adsorption, and they found that both the TPIM and KAUST-PI-1 membranes exhibited a typical hierarchical bimodal pore size distribution using N_2 molecules as the probe.[28,29]

3 Hierarchically microporous gas separation membranes

3.1 Polymers of intrinsic microporosity

Polymers of intrinsic microporosity (PIMs), which exhibit unprecedentedly high gas separation performance, have attracted significant attention since they were first developed in 2004 due to their characteristic ladder-type, contorted, and rigid polymer architectures enabling high microporosity.[30] Different PIMs have since then been developed with various structural considerations, such as PIM-1-based ladder polymers, PIM-polyimide (PIM-PI) polymers, and Tröger's base-based (PIM-TB) polymers (Fig. 2). Benchmarking PIM membranes in Robeson's upper bound plots[4,5] highlights their ultrahigh gas permeabilities compared with conventional polymer membranes; however, the gas selectivities of PIMs need to be improved. The relatively low gas selectivities of PIM membranes can be ascribed to the absence of well-defined microvoids, especially ultra-microcavities, which are crucial for size sieving. In this

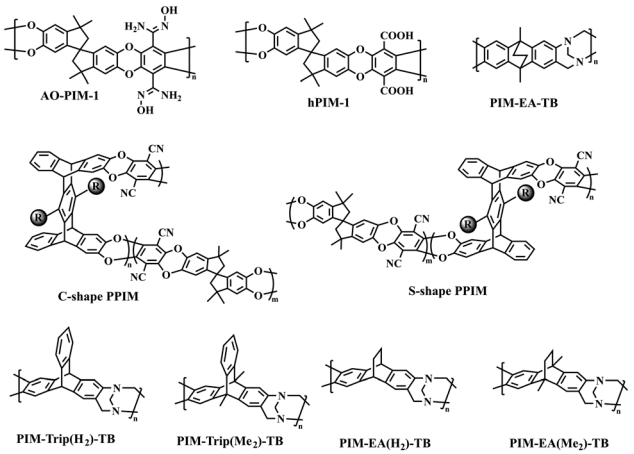

Fig. 2 Representative chemical structures of ladder-type PIMs.

regard, the fabrication of hierarchically microporous PIMs *via* pore manipulation strategies is of great importance.

PIM-1 is the most studied polymer for gas separations, and various approaches were developed to overcome its relatively low gas selectivity. For example, amidoxime-functionalized PIM-1 (AO-PIM-1, Fig. 2) was synthesized through the reaction between the nitrile groups and hydroxylamine, leading to a hierarchical microcavity size distribution with ultra-microporosity (<7 Å) as analyzed by low-temperature nitrogen adsorption using NLDFT micropore analysis, which led to a three-fold increase in CO_2/CH_4 selectivity compared to PIM-1.[31] A similar trend was observed for hydrolyzed PIM-1 membrane (hPIM-1, Fig. 2), which displayed a multimodal pore size distribution from the NLDFT analysis of N_2 adsorption isotherms at −196 °C,[32] and the CO_2/N_2 selectivity of the hPIM-1 membranes increased significantly with the increase of hydrolysis degree.[33] Additionally, direct fluorination of PIM-1 using a F_2/N_2 (5/95) gas mixture significantly improved size sieving due to the fluorine atom-induced pore blocking effect, and the fluorinated membranes also showed outstanding aging resistance.[34]

In addition to PIM-1 functionalization, novel ladder polymers of intrinsic microporosity were fabricated aiming at microcavity manipulation using either new PIM monomers or polymerization methods. Guo *et al.*[36] synthesized two pentiptycene-based PIM copolymers (PPIMs) with permanent and configurational free volume instilled by the shape-consistent pentiptycene moieties (Fig. 2). The as-prepared pentiptycene-based PIM membranes exhibited a typical bimodal micropore size distribution with two primary peaks at around 7–8 Å and 10–14 Å, respectively. The resulting hierarchical microcavity architecture enables superior gas separation performance far exceeding the 2008 upper bound and exceptional resistance to physical aging that often plagues high-free-volume PIMs. Luo *et al.*[37] reported a new macromolecular design of full-ladder polymers of intrinsic microporosity containing 9*H*-xanthene units (SACP-3) by superacid-catalyzed Friedel–Crafts polymerization. SACP-3 exhibited a bimodal micropore size distribution with two maxima at ~5 Å and ~8 Å (Fig. 3a). As a result, it showed a much higher CO_2 permeability of 6497 Barrer due to the more interconnected microporous structure, and the super rigid ladder structure enabled superior plasticization resistance unattainable in PIM-1. Xia *et al.* reported a novel class of hydrocarbon ladder polymers that displayed outstanding gas separation performance and aging resistance compared to conventional PIM membranes.[38] Particularly, the CANAL-Me-DHP membrane exhibited high H_2/CH_4 and CO_2/CH_4 selectivities of 621 and 68, respectively, with high H_2 and CO_2 permeabilities of 860 and 94 Barrer, respectively, after aging for 158 days. The profound effect of aging behavior was ascribed to the bottlenecks between free-volume elements narrowed down over time, leading to a more significant decrease in diffusion coefficients for larger gases. McKeown *et al.* fabricated novel PIMs containing spirocyclic units with fused triptycene, and the membranes exhibited a bimodal pore size distribution with a predominant ultra-microporosity size in the range of 5–7 Å and ultrahigh gas permeabilities.[39]

Tröger's base (TB)-based PIMs represent another type of high-performance gas separation membrane material due to the unique three-dimensional, V-shaped structure of Tröger's base, which has a characteristic twisting angle of 117° and can effectively disrupt polymer chain packing and generate high microporosity (Fig. 2).[40,41] Compared to PIM-1, PIM-EA-TB showed a bimodal micropore size distribution with higher chain rigidity, as evidenced by simulating their torsional angles.[42] Therefore, PIM-EA-TB exhibited higher size sieving and gas selectivities. Hu *et al.* synthesized four norbornyl bis-benzocyclobutene–Tröger's base polymers, and it was found that the *anti*-CANAL-4-MeNH_2-based TB polymer showed a unimodal pore size distribution, while the *syn*-CANAL-4-MeNH_2-based TB polymer displayed a bimodal pore size distribution.[43] Consequently, the *syn*-CANAL-4-MeNH_2-based TB polymer showed higher gas permeabilities and selectivities, and its gas separation performance for H_2/CH_4, H_2/N_2, and O_2/N_2 gas pairs approached the 2015 upper bounds.[6] Carta *et al.*[44] systematically investigated the microporosity and gas separation properties of four PIM-TB polymers, *e.g.*, PIM-Trip(H_2)-TB, PIM-Trip(Me_2)-TB, PIM-

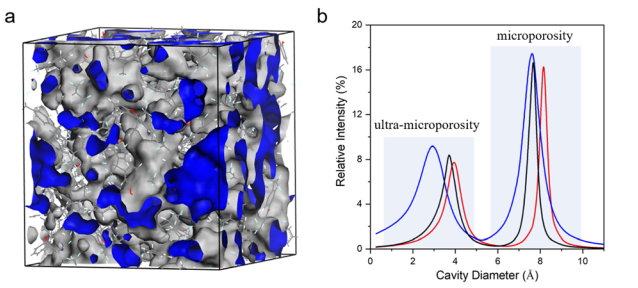

Fig. 3 (a) Modeling of micropore surfaces for a typical hierarchically microporous ladder polymer (reprinted with permission from ref. 35, Copyright (2022) Elsevier) and (b) pore size distribution of iptycene-based PI membranes (reprinted with permission from ref. 22, Copyright (2016) Elsevier).

EA(Me_2)-TB, and PIM-EA(H_2)-TB (Fig. 2). Interestingly, all PIM-TB membranes revealed a trimodal pore size distribution with the main pore sizes centered at around 3.5, 5.5, and 8.3 Å, respectively, confirming the enhancement of pore connectivity and consequently the superior gas separation performance. Pinnau *et al.* reported the synthesis of catalytic arene–norbornene annulation–Tröger's base ladder polymers (CANAL-TBs), which showed high BET surface areas of 900–1000 m^2 g^{-1} and a hierarchically bimodal pore size distribution.[45] The CANAL-TBs exhibited promising O_2/N_2 separation performance.

3.2 Polyimides and their derivatives

Polyimides (PIs) are arguably the most widely used membrane materials for gas separation, due to their outstanding mechanical strength, excellent thermal stability, high structural tunability, and attractive gas selectivities.[3] However, conventional polyimide membranes suffer from relatively low fractional free volumes and gas permeabilities, hindering their wide applications. Thus, various strategies were employed to manipulate the micropore structure to boost polyimides' gas separation performance, including novel bulky and rigid PI monomers, thermal rearrangement (TR), and thermal crosslinking. This section focuses on the recent progress in the development of microporous polyimides and their derivative membranes with tailored hierarchical microporous structures and the fundamental structure–property relationship.

Iptycenes are a family of bulky and rigid molecules composed of multiple benzene rings fused into a 3D configuration, among which triptycene and pentiptycene are the most frequently studied structure units to develop microporous membranes.[46] Incorporating iptycene moieties efficiently inhibit chain packing, enhancing the fractional free volume and micropore connectivity.[47,48] Additionally, the permanent configurational free volume elements delineated by the adjacent benzene rings exhibited comparable dimensions with the kinetic diameters of gas molecules, providing a unique strategy to finely tune the microporosity and enable high gas selectivities.[49,50] For instance, Luo *et al.*[47] synthesized a series of pentiptycene-based polyimides, which displayed bimodal micropore size distributions (6FDA-PPDA, Fig. 4). Compared to the corresponding triptycene-containing polyimides (6FDA-DAT1, Fig. 4), pentiptycene-based polyimide membranes showed higher FFVs and correspondingly higher gas permeabilities, and the microcavity could be finely modulated by different substituents (Fig. 3b). Notably, these iptycene-based polyimide membranes exhibited excellent resistance to physical aging or unusual aging-enhanced separation performance[51] due to the "stable" and accessible configurational free volumes generated by the shape-persistent iptycene units (Fig. 5a).[22,52]

Compared with PIM-1-based ladder polymers, PIM-PI polymers have also attracted much attention due to their

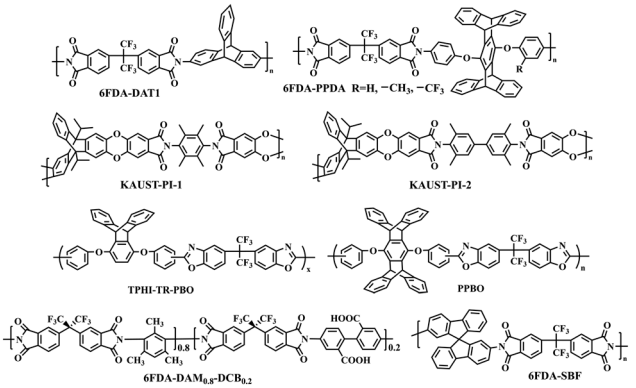

Fig. 4 Representative chemical structures of microporous polyimides and thermally rearranged (TR) polymers.

enhanced processability and excellent gas separation performance. Pinnau *et al.* fabricated KAUST-PIs (Fig. 4) containing the three-dimensional rigid triptycene moieties, and KAUST-PI-1 showed a super high BET surface area of 752 m^2 g^{-1}.[29] Notably, pore size distributions obtained from NLDFT analysis demonstrated a bimodal pore size distribution for both KAUST-PI-1 and KAUST-PI-2, and it was believed that interconnectivity induced by ultra-microporosity assisted molecule transport and united the high permeabilities with high selectivities for H_2/N_2, H_2/CH_4, and O_2/N_2 separations. This hierarchically microporous structure provided excellent gas separation performance with an H_2 permeability of 3983 Barrer and H_2/N_2 selectivity of 37 for KAUST-PI-1. Later on, KAUST-PI-1′ was fabricated by replacing 9,10-diisopropyl-substituted triptycenes with 9,10-dipropyl-substituted triptycenes, and the obtained KAUST-PI-1′ showed a similar bimodal pore size distribution.[53]

The development of high-performance polyimide membranes using other bulky structures was also reported. A spirobifluorene-containing polyimide (6FDA-SBF, Fig. 4) featuring intrinsic microporosity with a surface area of 550 m^2 g^{-1} was produced, and a multimodal pore size distribution was observed.[54] Yan *et al.* designed and synthesized dibenzodioxane-containing polyimides, and they all exhibited a bimodal pore size distribution characterized

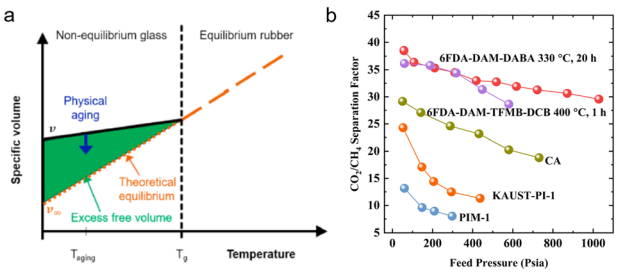

Fig. 5 (a) Physical aging of amorphous polymers (reprinted with permission from ref. 66, Copyright (2020) Elsevier) and (b) plasticization of typical crosslinked polyimide and PIM membranes (reprinted with permission from ref. 67, Copyright (2023) American Chemical Society).

by low-temperature N_2 adsorption.[55] Similarly, the 3D rigid dibenzodioxane moieties contributed to ultra-micropores (<7 Å), boosting their gas selectivities. Additionally, intrinsically microporous spirobifluorene-containing polyimides were designed and synthesized.[56] A significant increase in the number of ultra-micropores due to the shrinkage of larger micropores after aging for 200 days was observed, resulting in a dramatic enhancement of gas separation performance for O_2/N_2 and H_2/N_2 gas pairs.

Thermally rearranged (TR) polymers, which are generally produced by thermal treatment of *ortho*-functional (*e.g.*, hydroxyl, thiol, and amine) polyimide precursor membranes at elevated temperatures (300–450 °C) under inert conditions, are a highly attractive group of membrane materials that exhibit unprecedentedly high gas separation performance because of highly rigid and contorted backbone structures and high microporosity with hourglass-shaped architectures.[57] During the thermal rearrangement, an interconnected microcavity structure featuring a bimodal pore size distribution is generated. This leads to a significant enhancement of both permeability and selectivity compared to the polyimide precursors.[58] The microporosity and gas transport properties of TR polymers have been demonstrated to be highly tailorable *via* adjusting the precursor chemical structure or altering thermal treatment protocols.

Recent progress in TR polymers focuses on incorporating shape-persistent iptycene moieties to further tailor microporosity by introducing configurational free volume.[49,50,59,60] For example, triptycene-based TR polymers (TPHI-TR-PBO in Fig. 4) derived from THPI and ether-free triptycene-containing HPI exhibited significantly enhanced gas permeabilities for H_2/N_2, H_2/CH_4, and CO_2/CH_4 gas pairs.[50,59] More recently, a series of pentiptycene-based TR polymers (PPBO in Fig. 4) were reported, which demonstrated highly tailorable microporosity and, consequently, a broad range of separation performances *via* simply altering the TR protocols.[61] The impressive boosted gas separation performances were ascribed to the formation of well-defined microcavities during TR conversion in combination with the configurational free volume of iptycene units, as demonstrated by the increase in the population of microcavities (>7 Å) and negligible decrease in the population of ultra-microcavities (<7 Å). Later, new TR-able diamines such as adamantane[62] and fluorene-containing[63] hydroxyl diamines were designed to increase the TR conversion ratio and gas transport properties. Crosslinked TR polymers, which displayed the typical bimodal pore size distribution, were developed through simultaneous thermal rearrangement and crosslinking.[64,65] Notably, the population of micropores increased with increasing crosslinking degree, rendering a dramatic enhancement of gas permeabilities.

Conventional polyimide membranes are usually susceptible to plasticization due to polymer swelling upon adsorption of condensable gases, which results in severe deterioration of the mixed-gas CO_2/CH_4 selectivity for natural gas sweetening (Fig. 5b).[68] Thermally-induced chemical crosslinking of polyimide membranes has been widely implemented to suppress plasticization because it can appreciably regulate their microporosity and gas separation properties. Luo *et al.* developed a dual-thermally crosslinked strategy using a novel 4,4′-diamino-2,2′-biphenyldicarboxylic acid monomer.[24] The dual thermally crosslinked polyimide membranes displayed a hierarchically bimodal pore size distribution with ultra-micropores (2.0–6.0 Å) and micropores (6.5–10.0 Å) because of the collapse of segments and evolution of CO_2 during thermal treatment. The crosslinked membrane has superior plasticization resistance and mixed-gas separation performance to those of conventional non-crosslinkable polyimide membranes (Fig. 5b). Controllable thermal oxidative crosslinking was also recently reported to construct well-defined microcavities and crosslinked networks to boost gas separation and diminish plasticization.[40,69] Notably, a new crosslinked membrane design involving a model network structure formed by thermal end-linking of telechelic oligomers of precisely controlled molecular weight was reported.[70,71] In sharp contrast to traditional randomly crosslinked membranes, these crosslinked model network membranes showed an even higher gas permeability than their linear counterparts due to the model network design, and their separation performance was demonstrated to be highly tunable *via* simply adjusting the chain length of the telechelic oligomers, from which they were prepared.

3.3 Carbon molecular sieve membranes (CMSMs)

CMSMs, which are generally fabricated by carbonization of polymer precursors, display characteristic hierarchical microcavities and ultra-microcavities, thus exhibiting molecular sieving while allowing high gas permeabilities.[72] The representative turbostratic structure of CMSMs comprises graphene layers packed imperfectly, leading to slit-like micropores and ultra-micropores.[73] Pyrolysis has been considered the critical process for CMSM fabrication, which generates the microporous carbon structure necessary for molecular sieving. Various polymer precursors, including polyimides, polybenzimidazoles, phenolic resin, polyacrylonitrile (PAN), polyfurfuryl alcohol (PFA), PIMs, cellulose, polysulfones, *etc.*, have been fabricated into CMSMs *via* pyrolysis.[74] During this process, H_2 evolution forms a graphite-like structure and heteroatom elimination results in polymer chain rearrangement.[75] Therefore, the microporosity of CMSMs is primarily manipulated by the polymer precursors and the pyrolysis conditions such as the pyrolysis atmosphere, temperature, pyrolysis time, and ramp rate.

Among the pyrolysis conditions, the pyrolysis temperature plays a crucial role in regulating the microcavities. Generally, increasing the pyrolysis temperature increases crystallinity and reduces the average interplanar spacing, resulting in lower gas permeabilities and higher selectivities. This was evidenced by the weakening of the micropore peak (>5 Å) and the increase of the ultra-micropore peak (<5 Å),

providing evidence for the formation of ultramicropores at higher temperatures.[76] Besides, high ramping rates usually lead to pinholes and cracks, while low ramping rates result in higher carbon crystallinity and ultra-micropores.[77] Additionally, the pyrolysis atmosphere also affects the micropore structures. An oxidizing atmosphere typically enhances microporosity by degrading the precursors, yielding more open structures; an inert environment retains the microstructure and results in a tightly packed structure. Particularly, it was demonstrated that high-temperature H_2 exposure increased the CMS ultra-micropores, indicating that the high-temperature H_2 exposure can be used as post-synthesis modification to adjust the pore structure and the separation performance of CMS membranes.[78]

Besides the pyrolysis conditions, various post-treatment strategies, including post-oxidation, chemical vapor deposition, and post-pyrolysis, were employed to finely tune the microcavity size and distribution for demanding separation requirements.[79] Typically, post-oxidation or activation is frequently applied to increase the average micropore size when exposed to an oxidizing atmosphere. On the other hand, gas selectivities or molecule sieving of CMSMs can be enhanced by chemical vapor deposition (CVD), which introduces organic compounds into the micropore system and the pyrolytic decomposition.[80,81] Additionally, post-pyrolysis is another approach employed after post-oxidation to reduce micropore dimensions, and post-oxidation and post-pyrolysis are sometimes repeated alternately to achieve the desired micropore size distribution.

Ascribed to the hierarchically microporous architecture, CMSMs exhibit unprecedentedly high permselectivities far beyond the Robeson upper bounds for various crucial industrial gas separations such as natural gas sweetening (CO_2/CH_4), hydrogen recovery (H_2/N_2, H_2/CH_4), nitrogen removal from natural gas (N_2/CH_4), oxygen enrichment (O_2/N_2), and helium recovery from natural gas (He/CH_4),[82] as depicted in Fig. 6. Analysis of gas separation performance indicates that the ultrahigh gas selectivities originate from the constricted ultra-microcavities, which allow the permeation of small gases and exclude the transport of bulkier molecules.[83,84] Therefore, the precise control of micropore dimensions of CMSMs renders an efficient separation of gas mixtures even with slight size differences.

However, CMSMs always suffer from undesirable permeability/permeance loss, recognized as physical aging.[100] Physical aging is primarily caused by the initial imperfections of the graphene-like layers, making the CMSMs undergo gradual rearrangements to reach their thermodynamic equilibrium state. This is further evidenced by the decrease of the D/G ratio in Raman spectroscopy, revealing that the graphene-like layers of CMSMs are prone to rearrangement into a more ordered architecture.[101] Thereafter, various approaches, such as pre-crosslinking, post-crosslinking,[102] and polydimethylsiloxane (PDMS) coating,[103] were developed to mitigate the physical aging of CMSMs. For instance, the

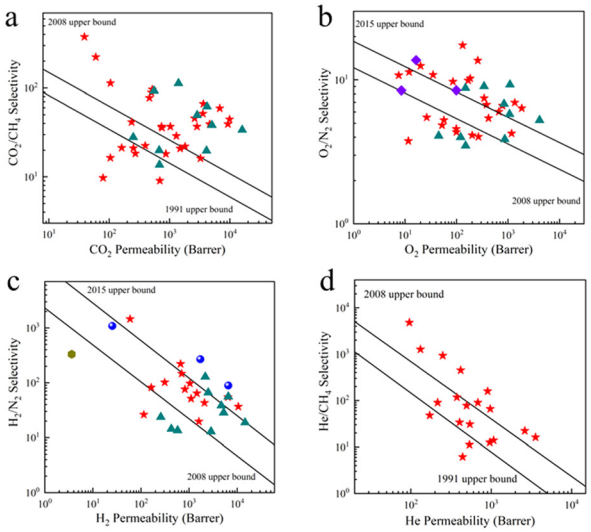

Fig. 6 Gas separation performance of CMS membranes for (a) CO_2/CH_4, (b) O_2/N_2, (c) H_2/N_2, and (d) He/CH_4 gas pairs. The red stars represent PI-based CMSMs,[78,85–94] navy spheres represent PIM-based CMSMs,[95,96] violet diamonds represent PBI-based CMSMs,[97] dark yellow hexagon represents PFA-based CMSMs,[98] and turquoise triangles represent polypyrrolone-based CMSMs.[99]

pre-crosslinking of polyimide precursors inhibited intersegmental motion and prevented the collapse of micropores, resulting in higher graphitic carbon content and less permeability reduction for the resulting CMSMs.[100] Despite numerous studies, limited success has been achieved in overcoming physical aging, and novel strategies are highly demanded to guarantee long-term stability. Additionally, low membrane strength has been the main obstacle limiting the wide application of CMSMs at the industrial level; therefore, novel CMSM fabrication methods, such as supported CMSMs, are needed to enhance membrane strength.

4 Conclusion and perspectives

This mini review systematically summarizes the recent progress on hierarchically microporous polymers, including highly microporous polymers of intrinsic microporosity, relatively less porous polyimides and their derivatives, and carbon molecular sieves, for high-performance gas separations. PIM functionalization, incorporation of hierarchical moieties such as iptycene, and chemical crosslinking are efficient approaches to constructing well-defined hierarchical architectures featuring both microporosity and ultra-microporosity with characteristic bimodal or multimodal pore size distributions. Hierarchical microporosity provides narrow necking for molecule sieving and micropore connectivity for fast gas transport, rendering significantly enhanced gas separation performance for various gas pairs compared to conventional polymer membranes with generally broad pore size distributions.

Despite the advantages of hierarchically microporous membranes, many novel materials and design approaches

are highly demanded to control micropore structures better and overcome the conventional upper bounds, providing directions for future research. To begin with, simulation and modeling at length scales from atomistic to continuum are crucial for understanding the basic structure–property relationship and offering rational guidance for the molecular-level design of future membranes. Secondly, pore engineering strategies such as anchoring functional groups to the micropore wall and incorporating crystalline structures to precisely manipulate the micropore size and architecture are highly demanded in future development. Developing novel membrane materials with diminished plasticization and physical aging would also expand their upscaling applications and boost membrane stabilities.

Conflicts of interest

The authors declare no conflict of interest.

Acknowledgements

S. Luo and S. Zhang gratefully acknowledge the financial support from the National Natural Science Foundation of China (22008243, 22090063, 21890760), the International Partner Program of CAS (122111KYSB20200035), and the Project of Stable Support for Youth Team in Basic Research Field of CAS (YSBR-017). R. Guo acknowledges the financial support from the Division of Chemical Sciences, Biosciences, and Geosciences, Office of Basic Energy Sciences of the U.S. Department of Energy (DOE), under award no. DE-SC0019024 and from the U.S. National Science Foundation under Cooperative Agreement No. EEC-1647722.

References

1 D. S. Sholl and R. P. Lively, Seven chemical separations to change the world, *Nature*, 2016, **532**, 435–437.
2 W. J. Koros and C. Zhang, Materials for next-generation molecularly selective synthetic membranes, *Nat. Mater.*, 2017, **16**, 289–297.
3 D. F. Sanders, Z. P. Smith, R. Guo, L. M. Robeson, J. E. McGrath, D. R. Paul and B. D. Freeman, Energy-efficient polymeric gas separation membranes for a sustainable future: A review, *Polymer*, 2013, **54**, 4729–4761.
4 L. M. Robeson, Correlation of separation factor versus permeability for polymeric membranes, *J. Membr. Sci.*, 1991, **62**, 165–185.
5 L. M. Robeson, The upper bound revisited, *J. Membr. Sci.*, 2008, **320**, 390–400.
6 R. Swaidan, B. Ghanem and I. Pinnau, Fine-tuned intrinsically ultramicroporous polymers redefine the permeability/selectivity upper bounds of membrane-based air and hydrogen separations, *ACS Macro Lett.*, 2015, **4**, 947–951.
7 B. Comesaña-Gándara, J. Chen, C. G. Bezzu, M. Carta, I. Rose, M.-C. Ferrari, E. Esposito, A. Fuoco, J. C. Jansen and N. B. McKeown, Redefining the Robeson upper bounds for CO_2/CH_4 and CO_2/N_2 separations using a series of ultrapermeable benzotriptycene-based polymers of intrinsic microporosity, *Energy Environ. Sci.*, 2019, **12**, 2733–2740.
8 H. B. Park, J. Kamcev, L. M. Robeson, M. Elimelech and B. D. Freeman, Maximizing the right stuff: The trade-off between membrane permeability and selectivity, *Science*, 2017, **356**, 6343.
9 Y. Peng, Y. Li, Y. Ban, H. Jin, W. Jiao, X. Liu and W. Yang, Membranes. Metal-organic framework nanosheets as building blocks for molecular sieving membranes, *Science*, 2014, **346**, 1356–1359.
10 S. Gao, Z. Li, Y. Yang, Z. Wang, Y. Wang, S. Luo, K. Yao, J. Qiu, H. Wang, L. Cao, Z. Lai and J. Wang, The ionic liquid–H_2O interface: A new platform for the synthesis of highly crystalline and molecular sieving covalent organic framework membranes, *ACS Appl. Mater. Interfaces*, 2021, **13**, 36507–36516.
11 A. A. Shamsabadi, M. Rezakazemi, F. Seidi, H. Riazi, T. Aminabhavi and M. Soroush, Next generation polymers of intrinsic microporosity with tunable moieties for ultrahigh permeation and precise molecular CO_2 separation, *Prog. Energy Combust. Sci.*, 2021, **84**, 100903.
12 Y. Wang, B. S. Ghanem, Z. Ali, K. Hazazi, Y. Han and I. Pinnau, Recent progress on polymers of intrinsic microporosity and thermally modified analogue materials for membrane-based fluid separations, *Small Struct.*, 2021, **2**, 2170026.
13 Y. Wang, B. S. Ghanem, Y. Han and I. Pinnau, State-of-the-art polymers of intrinsic microporosity for high-performance gas separation membranes, *Curr. Opin. Chem. Eng.*, 2022, **36**, 100755.
14 D. Kozono, M. Yasui, L. S. King and P. Agre, Aquaporin water channels: atomic structure and molecular dynamics meet clinical medicine, *J. Clin. Invest.*, 2002, **109**, 1395–1399.
15 S. Gravelle, L. Joly, F. Detcheverry, C. Ybert, C. Cottin-Bizonne and L. Bocquet, Optimizing water permeability through the hourglass shape of aquaporins, *Proc. Natl. Acad. Sci. U. S. A.*, 2013, **110**, 16367–16372.
16 H. J. Zhang, S. Sellaiyan, T. Kakizaki, A. Uedono, Y. Taniguchi and K. Hayashi, Effect of free-volume holes on dynamic mechanical properties of epoxy resins for carbon-fiber-reinforced polymers, *Macromolecules*, 2017, **50**, 3933–3942.
17 H. P. Degischer and B. Kriszt, Book review: Handbook of porous solids, *Adv. Mater.*, 2003, **15**, 1770–1771.
18 Y. P. Yampolskii, M. V. Motyakin, A. M. Wasserman, T. Masuda, M. Teraguchi, V. S. Khotimskii and B. D. Freeman, Study of high permeability polymers by means of the spin probe technique, *Polymer*, 1999, **40**, 1745–1752.
19 Y. P. Yampolskii, N. Kaliuzhnyi and S. Durgar'yan, Thermodynamics of sorption in glassy poly (vinyltrimethylsilane), *Macromolecules*, 1986, **19**, 846–850.
20 D. Hofmann, M. Heuchel, Y. Yampolskii, V. Khotimskii and V. Shantarovich, Free volume distributions in ultrahigh and

lower free volume polymers: Comparison between molecular modeling and positron lifetime studies, *Macromolecules*, 2002, **35**, 2129–2140.

21 Y. C. Jean, J. D. Van Horn, W.-S. Hung and K.-R. Lee, Perspective of positron annihilation spectroscopy in polymers, *Macromolecules*, 2013, **46**, 7133–7145.

22 S. Luo, J. R. Wiegand, P. Gao, C. M. Doherty, A. J. Hill and R. Guo, Molecular origins of fast and selective gas transport in pentiptycene-containing polyimide membranes and their physical aging behavior, *J. Membr. Sci.*, 2016, **518**, 100–109.

23 S. H. Han, N. Misdan, S. Kim, C. M. Doherty, A. J. Hill and Y. M. Lee, Thermally rearranged (TR) polybenzoxazole: Effects of diverse imidization routes on physical properties and gas transport behaviors, *Macromolecules*, 2010, **43**, 7657–7667.

24 C. Wang, Z. Cai, W. Xie, Y. Jiao, L. Liu, L. Gong, Q.-W. Zhang, X. Ma, H. Zhang and S. Luo, Finely tuning the microporosity in dual thermally crosslinked polyimide membranes for plasticization resistance gas separations, *J. Membr. Sci.*, 2022, **659**, 120769.

25 Y. G. Ptushinskiĭ, Low-temperature adsorption of gases on metal surfaces (Review), *Low Temp. Phys.*, 2004, **30**, 1–26.

26 J. Goworek, A. Borówka and R. Zaleski, Migration of siloxane polymer in ordered mesoporous MCM-41 silica channels, *Stud. Surf. Sci. Catal.*, 2007, **160**, 431–437.

27 S. Luo, Q. Zhang, Y. Zhang, K. P. Weaver, W. A. Phillip and R. Guo, Facile synthesis of a pentiptycene-based highly microporous organic polymer for gas storage and water treatment, *ACS Appl. Mater. Interfaces*, 2018, **10**, 15174–15182.

28 B. S. Ghanem, R. Swaidan, X. Ma, E. Litwiller and I. Pinnau, Energy-efficient hydrogen separation by AB-type ladder-polymer molecular sieves, *Adv. Mater.*, 2014, **26**, 6696–6700.

29 B. S. Ghanem, R. Swaidan, E. Litwiller and I. Pinnau, Ultra-microporous triptycene-based polyimide membranes for high-performance gas separation, *Adv. Mater.*, 2014, **26**, 3688–3692.

30 P. M. Budd, E. S. Elabas, B. S. Ghanem, S. Makhseed, N. B. McKeown, K. J. Msayib, C. E. Tattershall and D. Wang, Solution-processed, organophilic membrane derived from a polymer of intrinsic microporosity, *Adv. Mater.*, 2004, **16**, 456–459.

31 R. Swaidan, B. S. Ghanem, E. Litwiller and I. Pinnau, Pure- and mixed-gas CO_2/CH_4 separation properties of PIM-1 and an amidoxime-functionalized PIM-1, *J. Membr. Sci.*, 2014, **457**, 95–102.

32 Z. Hu, Y. Wang, X. Wang, L. Zhai and D. Zhao, Solution-reprocessable microporous polymeric adsorbents for carbon dioxide capture, *AIChE J.*, 2018, **64**, 3376–3389.

33 N. Du, G. P. Robertson, J. Song, I. Pinnau and M. D. Guiver, High-performance carboxylated polymers of intrinsic microporosity (PIMs) with tunable gas transport properties, *Macromolecules*, 2009, **42**, 6038–6043.

34 X. Ma, K. Li, Z. Zhu, H. Dong, J. Lv, Y. Wang, I. Pinnau, J. Li, B. Chen and Y. Han, High-performance polymer molecular sieve membranes prepared by direct fluorination for efficient helium enrichment, *J. Mater. Chem. A*, 2021, **9**, 18313–18322.

35 Z. Cai, Y. Liu, C. Wang, W. Xie, Y. Jiao, L. Shan, P. Gao, H. Wang and S. Luo, Ladder polymers of intrinsic microporosity from superacid-catalyzed Friedel-Crafts polymerization for membrane gas separation, *J. Membr. Sci.*, 2022, **644**, 120115.

36 T. J. Corrado, Z. Huang, D. Huang, N. Wamble, T. Luo and R. Guo, Pentiptycene-based ladder polymers with configurational free volume for enhanced gas separation performance and physical aging resistance, *Proc. Natl. Acad. Sci. U. S. A.*, 2021, **118**, e2022204118.

37 Z. Cai, Y. Liu, C. Wang, W. Xie, Y. Jiao, L. Shan, P. Gao, H. Wang and S. Luo, Ladder polymers of intrinsic microporosity from superacid-catalyzed Friedel-Crafts polymerization for membrane gas separation, *J. Membr. Sci.*, 2022, **644**, 120115.

38 H. W. H. Lai, F. M. Benedetti, J. M. Ahn, A. M. Robinson, Y. Wang, I. Pinnau, Z. P. Smith and Y. Xia, Hydrocarbon ladder polymers with ultrahigh permselectivity for membrane gas separations, *Science*, 2022, **375**, 1390–1392.

39 C. G. Bezzu, A. Fuoco, E. Esposito, M. Monteleone, M. Longo, J. C. Jansen, G. S. Nichol and N. B. McKeown, Ultrapermeable polymers of intrinsic microporosity (PIMs) containing spirocyclic units with fused triptycenes, *Adv. Funct. Mater.*, 2021, **31**, 2104474.

40 X. Chen, Y. Fan, L. Wu, L. Zhang, D. Guan, C. Ma and N. Li, Ultra-selective molecular-sieving gas separation membranes enabled by multi-covalent-crosslinking of microporous polymer blends, *Nat. Commun.*, 2021, **12**, 6140.

41 R. Williams, L. A. Burt, E. Esposito, J. C. Jansen, E. Tocci, C. Rizzuto, M. Lanc, M. Carta and N. B. McKeown, A highly rigid and gas selective methanopentacene-based polymer of intrinsic microporosity derived from Troger's base polymerization, *J. Mater. Chem. A*, 2018, **6**, 5661–5667.

42 E. Tocci, L. De Lorenzo, P. Bernardo, G. Clarizia, F. Bazzarelli, N. B. Mckeown, M. Carta, R. Malpass-Evans, K. Friess and K. T. Pilnáček, Molecular modeling and gas permeation properties of a polymer of intrinsic microporosity composed of ethanoanthracene and Tröger's base units, *Macromolecules*, 2014, **47**, 7900–7916.

43 X. Hu, J. Miao, Y. Pang, J. Zhao, Y. Lu, H. Guo, Z. Wang and J. Yan, Synthesis, microstructures, and gas separation performance of norbornyl bis-benzocyclobutene-Tröger's base polymers derived from pure regioisomers, *Polym. Chem.*, 2022, **13**, 2842–2849.

44 R. Malpass-Evans, I. Rose, A. Fuoco, P. Bernardo, G. Clarizia, N. B. McKeown, J. C. Jansen and M. Carta, Effect of bridgehead methyl substituents on the gas permeability of Tröger's-base derived polymers of intrinsic microporosity, *Membranes*, 2020, **10**, 62.

45 X. Ma, H. W. H. Lai, Y. Wang, A. Alhazmi, Y. Xia and I. Pinnau, Facile synthesis and study of microporous catalytic arene-norbornene annulation–tröger's base ladder polymers for

membrane air separation, *ACS Macro Lett.*, 2020, **9**, 680–685.
46 Y. Jiang and C.-F. Chen, Recent developments in synthesis and applications of triptycene and pentiptycene derivatives, *Eur. J. Org. Chem.*, 2011, **2011**, 6377–6403.
47 S. Luo, Q. Liu, B. Zhang, J. R. Wiegand, B. D. Freeman and R. Guo, Pentiptycene-based polyimides with hierarchically controlled molecular cavity architecture for efficient membrane gas separation, *J. Membr. Sci.*, 2015, **480**, 20–30.
48 Y. J. Cho and H. B. Park, High performance polyimide with high internal free volume elements, *Macromol. Rapid Commun.*, 2011, **32**, 579–586.
49 S. Luo, Q. Zhang, L. Zhu, H. Lin, B. A. Kazanowska, C. M. Doherty, A. J. Hill, P. Gao and R. Guo, Highly selective and permeable microporous polymer membranes for hydrogen purification and CO_2 removal from natural gas, *Chem. Mater.*, 2018, **30**, 5322–5332.
50 S. Luo, J. Liu, H. Lin, B. A. Kazanowska, M. D. Hunckler, R. K. Roeder and R. Guo, Preparation and gas transport properties of triptycene-containing polybenzoxazole (PBO)-based polymers derived from thermal rearrangement (TR) and thermal cyclodehydration (TC) processes, *J. Mater. Chem. A*, 2016, **4**, 17050–17062.
51 J. R. Weidman, S. Luo, C. M. Doherty, A. J. Hill, P. Gao and R. Guo, Analysis of governing factors controlling gas transport through fresh and aged triptycene-based polyimide films, *J. Membr. Sci.*, 2017, **522**, 12–22.
52 A. A. Shamsabadi, F. Seidi, M. Nozari and M. Soroush, A new pentiptycene-based dianhydride and its high-free-volume polymer for carbon dioxide removal, *ChemSusChem*, 2018, **11**, 472–482.
53 R. Swaidan, M. Al-Saeedi, B. Ghanem, E. Litwiller and I. Pinnau, Rational design of intrinsically ultramicroporous polyimides containing bridgehead-substituted triptycene for highly selective and permeable gas separation membranes, *Macromolecules*, 2014, **47**, 5104–5114.
54 J. Weber, Q. Su, M. Antonietti and A. Thomas, Exploring polymers of intrinsic microporosity – Microporous, soluble polyamide and polyimide, *Macromol. Rapid Commun.*, 2007, **28**, 1871–1876.
55 X. Hu, Y. Pang, H. Mu, X. Meng, X. Wang, Z. Wang and J. Yan, Synthesis and gas separation performances of intrinsically microporous polyimides based on 4-methylcatechol-derived monomers, *J. Membr. Sci.*, 2021, **620**, 118825.
56 X. Ma, B. Ghanem, O. Salines, E. Litwiller and I. Pinnau, Synthesis and effect of physical aging on gas transport properties of a microporous polyimide derived from a novel spirobifluorene-based dianhydride, *ACS Macro Lett.*, 2015, **4**, 231–235.
57 H. B. Park, C. H. Jung, Y. M. Lee, A. J. Hill, S. J. Pas, S. T. Mudie, E. Van Wagner, B. D. Freeman and D. J. Cookson, Polymers with cavities tuned for fast selective transport of small molecules and ions, *Science*, 2007, **318**, 254–258.
58 S. Kim and Y. M. Lee, Thermally rearranged (TR) polymer membranes with nanoengineered cavities tuned for CO_2 separation, *J. Nanopart. Res.*, 2012, **14**, 949.
59 F. Alghunaimi, B. Ghanem, Y. Wang, O. Salinas, N. Alaslai and I. Pinnau, Synthesis and gas permeation properties of a novel thermally-rearranged polybenzoxazole made from an intrinsically microporous hydroxyl-functionalized triptycene-based polyimide precursor, *Polymer*, 2017, **121**, 9–16.
60 S. Luo, Q. Zhang, T. K. Bear, T. E. Curtis, R. K. Roeder, C. M. Doherty, A. J. Hill and R. Guo, Triptycene-containing poly(benzoxazole-co-imide) membranes with enhanced mechanical strength for high-performance gas separation, *J. Membr. Sci.*, 2018, **551**, 305–314.
61 Z. Huang, C. Yin, T. Corrado, S. Li, Q. Zhang and R. Guo, Microporous pentiptycene-based polymers with heterocyclic rings for high-performance gas separation membranes, *Chem. Mater.*, 2022, **34**, 2730–2742.
62 C. Aguilar-Lugo, C. Álvarez, Y. M. Lee, J. G. de la Campa and Á. E. Lozano, Thermally rearranged polybenzoxazoles containing bulky adamantyl groups from ortho-substituted precursor copolyimides, *Macromolecules*, 2018, **51**, 1605–1619.
63 Y. F. Yeong, H. Wang, K. Pallathadka Pramoda and T.-S. Chung, Thermal induced structural rearrangement of cardo-copolybenzoxazole membranes for enhanced gas transport properties, *J. Membr. Sci.*, 2012, **397–398**, 51–65.
64 M. Calle, H. J. Jo, C. M. Doherty, A. J. Hill and Y. M. Lee, Crosslinked thermally rearranged poly(benzoxazole-co-imide) membranes prepared from ortho-hydroxycopolyimides containing pendant carboxyl groups and gas separation properties, *Macromolecules*, 2015, **48**, 2603–2613.
65 M. Calle, C. M. Doherty, A. J. Hill and Y. M. Lee, Crosslinked thermally rearranged poly(benzoxazole-co-imide) membranes for gas separation, *Macromolecules*, 2013, **46**, 8179–8189.
66 M. M. Merrick, R. Sujanani and B. D. Freeman, Glassy polymers: Historical findings, membrane applications, and unresolved questions regarding physical aging, *Polymer*, 2020, **211**, 123176.
67 T. Han, Z. Cai, C. Wang, P. Zheng, Q. Wu, L. Liu, X. Liu, J. Weidman and S. Luo, Ionic microporous polymer membranes for advanced gas separations, *Ind. Eng. Chem. Res.*, 2023, **62**(4), 1764–1775.
68 A. Bos, I. G. M. Punt, M. Wessling and H. Strathmann, CO_2-induced plasticization phenomena in glassy polymers, *J. Membr. Sci.*, 1999, **155**, 67–78.
69 Q. Song, S. Cao, R. H. Pritchard, B. Ghalei, S. A. Al-Muhtaseb, E. M. Terentjev, A. K. Cheetham and E. Sivaniah, Controlled thermal oxidative crosslinking of polymers of intrinsic microporosity towards tunable molecular sieve membranes, *Nat. Commun.*, 2014, **5**, 4813.
70 S. Li, Z. Dai, T. Wang, Z. Huang and R. Guo, Pentiptycene-containing polybenzoxazole membranes with a crosslinked unimodal network structure for high-temperature hydrogen separations, *Chem. Mater.*, 2022, **34**, 9577–9588.
71 S. Li, H. McGinness, T. Wang and R. Guo, Crosslinked Matrimid®-like polyimide membranes with unimodal network structure for enhanced stability and gas separation performance, *Polymer*, 2021, **237**, 124323.

72 M. Omidvar, H. Nguyen, L. Huang, C. M. Doherty, A. J. Hill, C. M. Stafford, X. Feng, M. T. Swihart and H. Lin, Unexpectedly strong size-sieving ability in carbonized polybenzimidazole for membrane H_2/CO_2 separation, *ACS Appl. Mater. Interfaces*, 2019, **11**, 47365–47372.
73 R. Singh and W. J. Koros, Carbon molecular sieve membrane performance tuning by dual temperature secondary oxygen doping (DTSOD), *J. Membr. Sci.*, 2013, **427**, 472–478.
74 S. J. Kim, Y. Kwon, D. Kim, H. Park, Y. H. Cho, S. E. Nam and Y. I. Park, A review on polymer precursors of carbon molecular sieve membranes for olefin/paraffin separation, *Membranes*, 2021, **11**, 482.
75 W. N. W. Salleh, A. F. Ismail, T. Matsuura and M. S. Abdullah, Precursor selection and process conditions in the preparation of carbon membrane for gas separation: A review, *Sep. Purif. Rev.*, 2011, **40**, 261–311.
76 L. Liu, D. X. Liu and C. Zhang, High-temperature hydrogen/propane separations in asymmetric carbon molecular sieve hollow fiber membranes, *J. Membr. Sci.*, 2022, **642**, 119978.
77 W. N. W. Salleh and A. F. Ismail, Effects of carbonization heating rate on CO_2 separation of derived carbon membranes, *Sep. Purif. Technol.*, 2012, **88**, 174–183.
78 E. P. Fawas, G. C. Kapantaidakis, J. W. Nolan, A. C. Mitropoulos and N. K. Kanellopoulos, Preparation, characterization and gas permeation properties of carbon hollow fiber membranes based on Matrimid (R) 5218 precursor, *J. Mater. Process. Technol.*, 2007, **186**, 102–110.
79 C. H. Liang, G. Y. Sha and S. C. Guo, Carbon membrane for gas separation derived from coal tar pitch, *Carbon*, 1999, **37**, 1391–1397.
80 J.-i. Hayashi, M. Yamamoto, K. Kusakabe and S. Morooka, Simultaneous improvement of permeance and permselectivity of 3, 3′, 4, 4′-biphenyltetracarboxylic dianhydride-4, 4′-oxydianiline polyimide membrane by carbonization, *Ind. Eng. Chem. Res.*, 1995, **34**, 4364–4370.
81 A. Cabrera, J. Zehner, C. Coe, T. Gaffney, T. Farris and J. Armor, Preparation of carbon molecular sieves, I. Two-step hydrocarbon deposition with a single hydrocarbon, *Carbon*, 1993, **31**, 969–976.
82 C. Zhang and W. J. Koros, Ultraselective carbon molecular sieve membranes with tailored synergistic sorption selective properties, *Adv. Mater.*, 2017, **29**, 1701631.
83 L.-H. Cheng, Y.-J. Fu, K.-S. Liao, J.-T. Chen, C.-C. Hu, W.-S. Hung, K.-R. Lee and J.-Y. Lai, A high-permeance supported carbon molecular sieve membrane fabricated by plasma-enhanced chemical vapor deposition followed by carbonization for CO_2 capture, *J. Membr. Sci.*, 2014, **460**, 1–8.
84 W. Salleh and A. F. Ismail, Carbon membranes for gas separation processes: Recent progress and future perspective, *J. Membr. Sci. Res.*, 2015, **1**, 2–15.
85 C.-P. Hu, C. K. Polintan, L. L. Tayo, S.-C. Chou, H.-A. Tsai, W.-S. Hung, C.-C. Hu, K.-R. Lee and J.-Y. Lai, The gas separation performance adjustment of carbon molecular sieve membrane depending on the chain rigidity and free volume characteristic of the polymeric precursor, *Carbon*, 2019, **143**, 343–351.
86 K. Hazazi, X. Ma, Y. Wang, W. Ogieglo, A. Alhazmi, Y. Han and I. Pinnau, Ultra-selective carbon molecular sieve membranes for natural gas separations based on a carbon-rich intrinsically microporous polyimide precursor, *J. Membr. Sci.*, 2019, **585**, 1–9.
87 Q. Wang, F. Huang, C. J. Cornelius and Y. Fan, Carbon molecular sieve membranes derived from crosslinkable polyimides for CO_2/CH_4 and C_2H_4/C_2H_6 separations, *J. Membr. Sci.*, 2021, **621**, 118785.
88 K. Li, Z. Zhu, H. Dong, Q. Li, W. Ji, J. Li, B. Cheng and X. Ma, Bottom up approach to study the gas separation properties of PIM-PIs and its derived CMSMs by isomer monomers, *J. Membr. Sci.*, 2021, **635**, 119519.
89 P. S. Tin, T. S. Chung, Y. Liu and R. Wang, Separation of CO_2/CH_4 through carbon molecular sieve membranes derived from P84 polyimide, *Carbon*, 2004, **42**, 3123–3131.
90 B. T. Low and T. S. Chung, Carbon molecular sieve membranes derived from pseudo-interpenetrating polymer networks for gas separation and carbon capture, *Carbon*, 2011, **49**, 2104–2112.
91 L. Shao, T. S. Chung, G. Wensley, S. H. Goh and K. P. Pramoda, Casting solvent effects on morphologies, gas transport properties of a novel 6FDA/PMDA-TMMDA copolyimide membrane and its derived carbon membranes, *J. Membr. Sci.*, 2004, **244**, 77–87.
92 N. Widiastuti, A. R. Widyanto, I. S. Caralin, T. Gunawan, R. Wijiyanti, W. N. W. Salleh, A. F. Ismail, M. Nomura and K. Suzuki, Development of a P84/ZCC composite carbon membrane for gas separation of H_2/CO_2 and H_2/CH_4, *ACS Omega*, 2021, **6**, 15637–15650.
93 H. Suda and K. Haraya, Gas permeation through micropores of carbon molecular sieve membranes derived from Kapton polyimide, *J. Phys. Chem. B*, 1997, **101**, 3988–3994.
94 Y. Xiao, Y. Dai, T.-S. Chung and M. D. Guiver, Effects of brominating Matrimid polyimide on the physical and gas transport properties of derived carbon membranes, *Macromolecules*, 2005, **38**, 10042–10049.
95 Z. Wang, H. Ren, S. Zhang, F. Zhang and J. Jin, Carbon molecular sieve membranes derived from Troger's base-based microporous polyimide for gas separation, *ChemSusChem*, 2018, **11**, 916–923.
96 X. Ma, R. Swaidan, B. Teng, H. Tan, O. Salinas, E. Litwiller, Y. Han and I. Pinnau, Carbon molecular sieve gas separation membranes based on an intrinsically microporous polyimide precursor, *Carbon*, 2013, **62**, 88–96.
97 J. G. Seong, J. C. Lewis, J. A. Matteson, E. Craddock, U. Martinez, H. Thakkar, A. D. Benavidez, K. A. Berchtold and R. P. Singh, Polybenzimidazole-derived carbon molecular sieve hollow fiber membranes with tailored oxygen selective transport, *Carbon*, 2022, **192**, 71–83.
98 M. B. Shiflett and H. C. Foley, Ultrasonic deposition of high-selectivity nanoporous carbon membranes, *Science*, 1999, **285**, 1902–1905.

99 H. Kita, M. Yoshino, K. Tanaka and K.-i. Okamoto, Gas permselectivity of carbonized polypyrrolone membrane, *Chem. Commun.*, 1997, 1051–1052.

100 C. Karunaweera, I. H. Musselman, K. J. Balkus, Jr. and J. P. Ferraris, Fabrication and characterization of aging resistant carbon molecular sieve membranes for C-3 separation using high molecular weight crosslinkable polyimide, 6FDA-DABA, *J. Membr. Sci.*, 2019, **581**, 430–438.

101 X. Ma, S. Williams, X. Wei, J. Kniep and Y. Lin, Propylene/propane mixture separation characteristics and stability of carbon molecular sieve membranes, *Ind. Eng. Chem. Res.*, 2015, **54**, 9824–9831.

102 G. B. Wenz and W. J. Koros, Tuning carbon molecular sieves for natural gas separations: A diamine molecular approach, *AIChE J.*, 2017, **63**, 751–760.

103 J. H. Shin, H. J. Yu, H. An, A. S. Lee, S. S. Hwang, S. Y. Lee and J. S. Lee, Rigid double-stranded siloxane-induced high-flux carbon molecular sieve hollow fiber membranes for CO_2/CH_4 separation, *J. Membr. Sci.*, 2019, **570**, 504–512.